Colloid Polym Sci 279:1192–1199 (2001)
© Springer-Verlag 2001

ORIGINAL CONTRIBUTION

P. Gasbarrone
C. La Mesa

Interactions of short-chain surfactants with a nonionic polymer

Received: 28 February 2001
Accepted: 5 June 2001

P. Gasbarrone · C. La Mesa (✉)
Dipartimento di Chimica
Università di Roma La Sapienza
P. le A. Moro 5, 00185 Rome, Italy
e-mail: camillo.lamesa@uniroma1.it

Abstract Aqueous solutions containing poly(vinylpyrrolidone) (PVP) and sodium caprylate (SCAP) or tetraethylammonium perfluorooctanesulfonate have been investigated as a function of the surfactant content, the added polymer, temperature and ionic strength. According to experimental evidence, significant interactions have been observed in both systems, with the occurrence of both critical association and micelle formation thresholds. Volumetric, viscometric, ionic conductivity and surface tension methods have been used to quantify the interactions between surfactants and the polymer in ternary systems containing PVP and SCAP or the polymer and the fluorinated surfactant. In both cases, the width of the interaction region is proportional to the PVP content in the mixture. Temperature and ionic strength have a relevant effect on the width of the interaction region, which decreases on increasing the temperature. Binding onto PVP and micelle formation were analyzed in terms of a mass-action model. In this way, the observed behavior was rationalized and information on the thermodynamics of such mixtures was given.

Key words Surfactants · Polymers · Interactions · Polymer–surfactant complexes · Thermodynamics

Introduction

Systems containing polymers and surfactants are the subject of significant research interest [1–4, 5]. The possible technological applications of these systems, in fact, justify experimental investigation of their physicochemical properties [6–9] as well as theoretical modeling [10–15]. Such studies have consequences for fundamental and applied aspects of these systems, for instance, in explaining the peculiar phenomena involved in the solubilization, adsorption and rheology of polymer–surfactant systems.

Most of the investigations reported so far concern the interactions between neutral homopolymers [poly(ethylene glycol), poly(ethylene oxide) or poly (vinylpyrrolidone) (PVP)] and sodium dodecyl sulfate or dodecyltrimethylammonium bromide [16, 17]. More recently, the interactions between block copolymers and surface-active agents [18], between surfactants and polyelectrolytes [19, 20] or selected proteins [21, 22] have also been discussed.

Not much is known about the interactions between homopolymers and short-chain surfactants. It has been known for a long time that some of them do not interact with homopolymers [3, 7]. Information on this, unfortunately, is poor; thus, detailed knowledge of all the factors controlling polymer–surfactant interactions in systems containing short-chain surfactants is required.

To shed light on this subject, we investigated some physicochemical properties of aqueous PVP and sodium caprylate (SCAP), PVP in 1 m aqueous NaCl and sodium caprylate and aqueous PVP and tetraethylammonium perfluorooctanesulfonate (TEAPFOSS).

A detailed analysis on the interactions between the polymer and the aforementioned surfactants was used to clarify some aspects, in particular the replacement of polymethylene chains with fluorinated ones, as well as the role that temperature and ionic strength exert on polymer–surfactant interactions.

Information on the forces controlling polymer–surfactant interactions was inferred from thermodynamic and transport properties. A thermodynamic analysis of such interactions, based on a mass-action model, was used by some of us in the analysis of the kinetics of polymer–surfactant interactions [11, 13, 17, 23]. With some formal changes, the model is applied to the PVP–SCAP, and PVP–TEAPFOSS systems.

Experimental

Materials

Ethanol, NaCl, HCl, absolute ethanol and sodium (used in the preparation of sodium ethoxide) were from Aldrich. NaCl was vacuum dried before use. Deionized and doubly distilled water, ($\kappa \approx 1$ μS at 25 °C) was used.

SCAP, caprylic acid and TEAPFOSS, nominal purity higher than 98%, were from Aldrich. Foaming fractionation was used to purify the surfactants [24]. Application of this technique to SCAPwas not satisfactory. Thus, titration of caprylic acid with sodium ethoxide in hot ethanol was performed. The solution resulting from the titration in the ethanolic medium was concentrated and the solid was dried in a vacuum. Foaming of its diluted aqueous solutions (at a concentration below the critical micelle concentration, cmc) was used. As inferred from the surface tension versus logm plots, the product does not show significant surface-active impurities.

PVP, average molecular mass, <Mw>, of 28 kDa, (Aldrich), was used. Cartridges (Nuclepore, 800 μm) were used to filter the polymer-containing solutions, to remove dust and large particles.

The solutions were prepared by weight and were corrected for buoyancy.

Methods

Surface properties

A K10T unit (Kruss), thermostatted to 0.1 °C by circulating water, was used to measure the surface tension, σ. Details of the calibration and the measuring procedures are given elsewhere [25]. The platinum Du Noüy ring was roasted in a red flame, washed in 0.1 m HCl and cleaned in doubly distilled water. The surface tension of the conductivity water was 71.8 $\mathrm{mNm^{-1}}$ at 25 °C.

The σ values were obtained from five or more independent determinations, with an accuracy of $\pm 0.3\ \mathrm{mNm^{-1}}$. The data were analyzed using the Gibbs adsorption isotherm

$$d\sigma = -\Gamma_2[2RTd\ln a_2] \approx -\Gamma_2[2RTd\ln m_2] \ , \tag{1}$$

where T is the temperature, Γ_2 the surface-excess concentration and R is the gas constant. The solute activity, a_2, was replaced by the corresponding molality, m_2.

Viscosity

The viscosity, η, was measured using Ubbelhode viscometers (Schott). To minimize spurious kinetic effects, the viscometers had flow times in the range 2–300 s. The accuracy was to 0.2 s. Each datum is the result of at least five determinations. The relative viscosity, η_{rel}, was calculated from

$$\eta_{rel} = \eta/\eta^{\circ} = (t\rho/t^0\rho^0) \ , \tag{2}$$

where t and t^0 are the solution and solvent flow times, respectively, and ρ and ρ^0 are the corresponding densities.

Selected relative viscosity data are reported in Table 1.

Volumetric properties

The solution density, ρ, was measured using a DMA 60 vibration densimeter (Anton Paar), thermostatted to within ±0.002 °C by a circulating water bath (Heto). The uncertainty in ρ was $\pm 2 \times 10^{-6}\ \mathrm{gcm^{-3}}$. Apparent, $\Phi_{V,2}$, and partial, V_2, molal volumes were obtained from the relations

$$\Phi_{V,2} = MW/\rho - 10^3(\rho - \rho^0)/\rho\rho^0 m_2 \ , \tag{3}$$

$$V_2 = \partial(m_2\Phi_{V,2})/\partial m_2 \ , \tag{4}$$

Table 1 The surfactant molality, m, and the relative viscosity, η_{rel}, of the system water–poly(vinylpyrrolidone) (PVP)–sodium caprylate at 25 °C

H_2O		0.1 wt% PVP		0.2 wt% PVP		0.3 wt% PVP		0.5 wt% PVP	
m	η_{rel}	m	η_{rel}	m	η_{rel}	m	η_{rel}	m	η_{rel}
0.0639	1.051	0.0803	1.047	0.0500	1.097	0.1559	1.118	0.1679	1.149
0.148	1.119	0.1559	1.118	0.1496	1.190	0.2312	1.183	0.2481	1.224
0.218	1.162	0.2312	1.183	0.1904	1.235	0.2912	1.217	0.3077	1.312
0.299	1.232	0.2619	1.224	0.2523	1.301	0.2989	1.268	0.3610	1.339
0.348	1.276	0.2989	1.291	0.2977	1.326	0.3380	1.270	0.3938	1.317
0.431	1.353	0.3380	1.317	0.3481	1.364	0.3755	1.328	0.4606	1.380
0.544	1.456	0.3756	1.329	0.4045	1.391	0.4177	1.326	0.4984	1.352
0.670	1.626	0.4178	1.349	0.4452	1.413	0.4548	1.398	0.5652	1.419
0.766	1.796	0.4548	1.351	0.5021	1.427	0.5000	1.442	0.6541	1.467
0.876	1.963	0.5003	1.366	0.5378	1.430	0.6247	1.493	0.7135	1.753
0.933	2.084	0.5670	1.466	0.5988	1.506	0.7490	1.748	0.7977	1.860
1.05	2.284	0.6247	1.592	0.6928	1.777	0.8485	1.934	0.8565	1.940
		0.6940	1.715	0.7838	1.875	0.9959	1.934	0.9130	2.063
		0.8486	1.934	0.8823	2.039		2.227	0.9946	2.212
		0.9960	2.211	0.9677	2.198				
				1.0319	2.434				

where MW is the solute molal mass and the other symbols are as previously. The apparent and the partial molal volumes are given in Table 2 and in Fig. 1, respectively.

Electrical conductance

A 730 Amel unit, equipped with a small-volume conductivity cell, was used to measure the electrical conductance, κ. The cell was thermostatted to ± 0.002 °C by circulating oil. An F25 precision thermometer (Automatic System Laboratories) was used to measure the temperature. When polymer–surfactant interactions were present two changes in the slope were observed (Fig. 2). From the data critical association concentration (cac) and cmc* values [7, 8, 9, 26] were obtained.

Results

Volumetric properties

The volumetric behavior of the water–PVP–SCAP system is quite different from the water–SCAP one, as indicated in Fig. 1. The volume change of the micelle formation, ΔV_{mic}, (11 cm^3mol^{-1}), was evaluated from the distance between the tangents to the two branches of the curve at the cmc [27]. The volume change associated with the polymer–surfactant interactions, ΔV_{psi} (8–9 cm^3mol^{-1}), was calculated in the same way. Its value is slightly dependent on the PVP content. As expected, ΔV_{psi} is lower than ΔV_{mic}.

Table 2 The molality, m ($molkg^{-1}$), and the apparent molal volume, $\Phi_{V,2}$ (cm^3mol^{-1}), of sodium caprylate in water and in 1.003 wt% PVP at 25 °C

m	$\Phi_{V,2}$	m	$\Phi_{V,2}$
Water			
2.51×10^{-2}	132.1	5.12×10^{-1}	136.4
5.11×10^{-2}	132.1	5.53×10^{-1}	137.0
1.15×10^{-1}	132.2	6.11×10^{-1}	137.5
1.54×10^{-1}	132.4	6.52×10^{-1}	138.0
2.04×10^{-1}	132.7	7.13×10^{-1}	138.2
2.53×10^{-1}	133.3	7.52×10^{-1}	138.4
3.02×10^{-1}	133.7	8.03×10^{-1}	138.6
3.52×10^{-1}	134.2	8.51×10^{-1}	138.7
4.01×10^{-1}	134.0	9.02×10^{-1}	138.9
4.53×10^{-1}	135.7	9.54×10^{-1}	139.0
4.87×10^{-1}	136.0	1.05×10^{0}	139.2
1.003 wt% PVP			
2.31×10^{-2}	130.1	5.72×10^{-1}	134.0
5.22×10^{-2}	130.1	6.03×10^{-1}	135.1
1.11×10^{-1}	130.2	6.48×10^{-1}	135.9
1.55×10^{-1}	130.4	7.02×10^{-1}	136.6
2.13×10^{-1}	130.7	7.63×10^{-1}	137.1
2.50×10^{-1}	130.9	8.00×10^{-1}	137.7
3.00×10^{-1}	131.3	8.48×10^{-1}	137.9
3.48×10^{-1}	131.5	9.11×10^{-1}	138.0
4.11×10^{-1}	132.0	9.51×10^{-1}	138.2
4.57×10^{-1}	132.4	1.01×10^{-1}	138.4
4.82×10^{-1}	133.1	1.25×10^{0}	138.7
5.09×10^{-1}	133.6	1.46×10^{0}	138.9

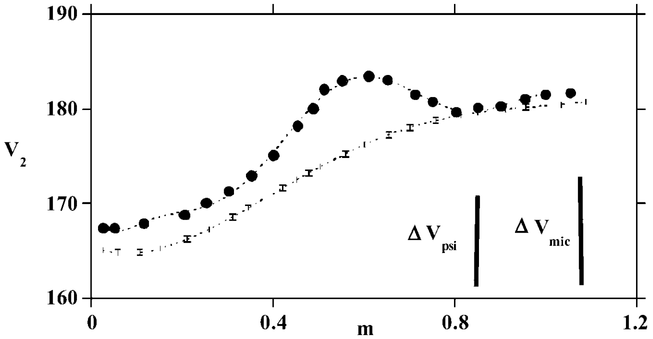

Fig. 1 Partial molal volume, V_2 (cm^3mol^{-1}), of sodium caprylate (SCAP) in water (full symbols) and in 1 wt % poly(vinylpyrrolidone) (PVP), as a function of molality at 25 °C. The volume changes of micelle formation, ΔV_{mic}, and of polymer–surfactant interactions, ΔV_{psi}, are indicated by bars on the right-hand side of the figure

The data in Fig. 1 indicate that the number-average aggregation numbers of polymer-bound aggregates are lower that those of free micelles. In the mass-action model for micelle formation, in fact, the slope of the $\Phi_{V,2}$ function around the transition concentration is proportional to the micelle aggregation number [28].

The following relation may be used to calculate $<m>$ and $<n>$ values, i.e. the number-average aggregation numbers of free and polymer-bound micelles, respectively [29],

$$\Phi_{V,2} = A(V_2^0 + AA_V m_2) + (1 - A)V_{2,\infty} \ , \quad (5)$$

where V_2^0 and $V_{2,\infty}$ are the lower and upper limits of the partial molal volume, respectively, the quantity A is the ratio between the molecular and the overall surfactant content and A_V is a parameter accounting for pairwise interactions between surfactant monomers [28].

Assuming that $\partial A^2/\partial m_2^2$ is zero at the cmc, or at the cac, the number-average aggregation number may be obtained from [29]

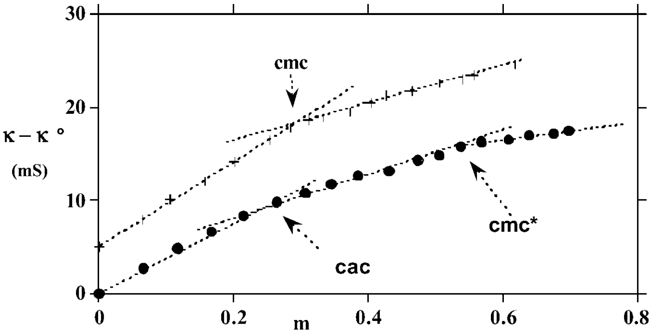

Fig. 2 Electrical conductance, κ–κ^0 (mS), as a function of caprylate molality in water (crosses) and in 1 wt %, PVP (full symbols) at 25 °C. To avoid overlapping, the former curve has been shifted 5 mS upward

$$A = (x/x - 1)[1 - (1/2x)^{1/2}] \ , \quad (6)$$

where x is either $<n>$ or $<m>$. In systems containing SCAP at 25 °C the number-average aggregation numbers decrease from about 18–20 (in water) to 12–13 in the presence of 1 wt% PVP. Within the limits set up by the approach, the values obtained by the fit are reasonable.

In the water–PVP–TEAPFOSS system the very low cac and cmc* values do not allow the volumetric behavior to be determined with due accuracy. Estimates indicate that ΔV_{mic} is close to 14 cm^3mol^{-1} [30]. The volume change associated with polymer–surfactant interactions, ΔV_{psi}, is about 11 cm^3mol^{-1}. This behavior (i.e. $\Delta V_{psi} < \Delta V_{mic}$) is in line with previous findings [31, 32] and is similar to that observed in dilution enthalpies [33, 34] and adiabatic compressibility [17, 35].

Electrical conductance

When polymer–surfactant interactions are present, the κ(m) curves show two distinct changes in slope (Fig. 2). Such changes are associated with the cac and with micelle formation, once the polymer binding sites have been saturated by the surfactant. The electrical conductance, unfortunately, does not allow us to ascertain whether the interactions are related to ion, or aggregate, binding onto the polymer.

Surface properties

When PVP is present two distinct changes in slope are observed (Fig. 3). They are related to the onset of polymer–surfactant interaction and to micelle formation, respectively. The distance between such points is proportional to the polymer weight percent in the mixture. The cac is slightly dependent on the polymer content in the solvent.

Solution viscosity

The Data in Table 1 and in Fig. 4 indicate the presence of two changes in slope at the cac and the cmc*, respectively. The aforementioned behavior depends on the PVP content, temperature and added electrolyte.

The limiting hydrodynamic volume of the surfactant molecule, V_η [36, 37], is inversely proportional to the amount of PVP in the solvent. This is a qualitative indication that polymer-bound aggregates are smaller than free micelles. Added NaCl and temperature have a pronounced effect on the hydrodynamic volume of free and polymer-bound aggregates.

Thermodynamic behavior

At 25 °C, the cmc of SCAP is 0.35 m [38] and that of TEAPFOSS is about 1 mm [30]. The micelle aggregation numbers are between 15 and 20, depending on the surfactant [39–41]. As indicated before, the presence of PVP shifts the micelle formation to higher values.

The Gibbs energy of micelle formation, $\Delta G_{mic} = RT\ln(cmc)$, and that associated with polymer–surfactant interactions, $\Delta G_{psi} = RT\ln(cac)$, are reported in Table 3. These quantities indicate the transfer of a surfactant molecule from the bulk to a micellelike interior or to a polymer binding site, respectively.

The nature of the surfactant, the PVP weight percent and the temperature control the free energy of transfer from a polymer binding site to the micelles, ΔG_{tr}. The related behavior is indicated in Fig. 5.

The enthalpies and entropies associated with polymer–surfactant interactions were obtained from the dependence of ΔG_{psi} on temperature and added PVP

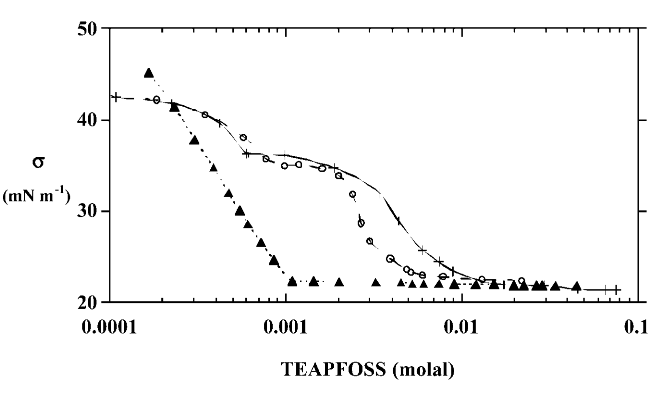

Fig. 3 Surface tension, σ (mNm^{-1}), as a function of the logarithm of the concentration of tetraethylammonium perfluorooctanesulfonate (TEAPFOSS) in water (triangles), 0.10 wt% PVP (circles) and 0.30 wt% PVP (crosses) at 25 °C

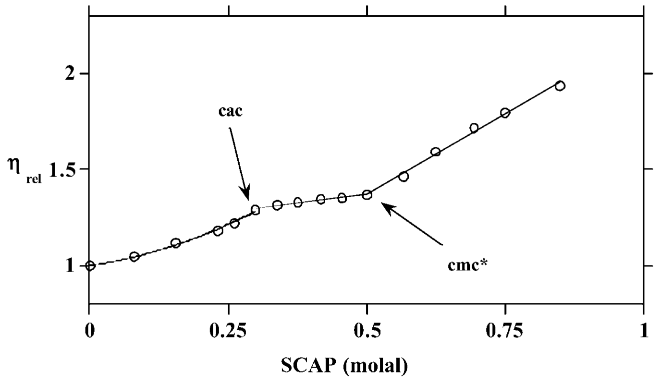

Fig. 4 Relative viscosity plots, η_{rel}, as a function of sodium caprylate molality for a systems containing 0.10 wt%, PVP at 25 °C

Table 3 The Gibbs energy associated with the critical association concentration (cac), RTln(cac) (kcalmol^{-1}), and that associated with micelle formation, RTln(cmc*) (kcalmol^{-1}), of sodium caprylate as a function of PVP weight percent at 25 °C

PVP (wt%)	RTln(cac)	RTln(cmc*)
0.10300	−13.2	−10.8
0.20100	−13.3	−10.6
0.29800	−13.4	−10.5
0.40400	−13.4	−10.4
0.50000	−13.5	−10.4
0.60700	−13.5	−10.3
0.74700	−13.6	−10.3
1.0030	−13.7	−10.2

Table 4 The enthalpic, ΔH_{psi} (kcalmol^{-1}), and entropic, ΔS_{psi} (calmol^{-1}deg^{-1}), contributions associated with polymer–surfactant interactions in the water–sodium caprylate–PVP system. ΔH_{psi} data were calculated from the temperature dependence of the cac in the temperature range 15–45 °C

PVP (wt%)	ΔH_{psi}	ΔS_{psi}
0.1031	1.84	3.4
0.2012	1.51	6.7
0.2980	1.07	10.2
0.4043	0.66	13.2
0.5001	0.27	16.8
0.6068	−0.23	20.2
0.7467	−0.89	23.5
1.003	−1.45	26.8

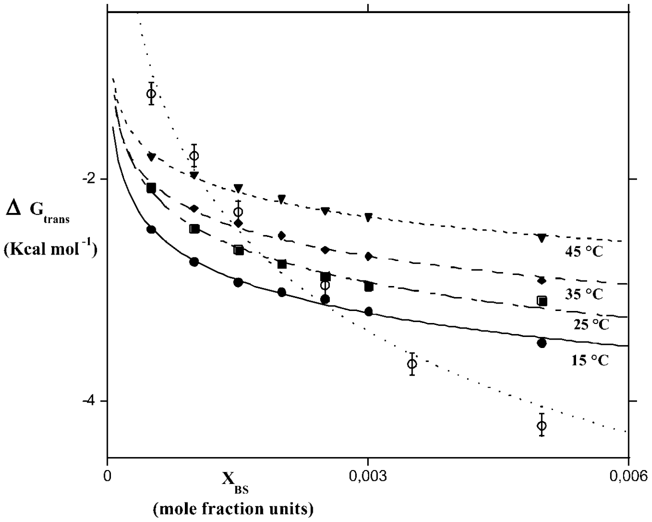

Fig. 5 RTln(cac/cmc) (kcalmol^{-1}) as a function of the mole fraction of polymer binding sites, X_{BS}, for TEAPFOSS (empty symbols) at 25 °C and SCAP (full symbols) at different temperatures

(Table 4). According to the data reported there, ΔH_{psi} is linearly dependent on the number of polymer binding sites and becomes progressively negative. As in the case of micelle formation, polymer–surfactant interactions are mainly controlled by entropic contributions. ΔS_{psi}, in fact, is almost linearly dependent on the mole fraction of polymer binding sites, $X_{3,BS}$. As in previous studies [23], the molar mass of the latter quantity was assumed to be about 2 kDa.

Discussion

Several thermodynamic contributions control the organization of amphiphiles into micelles (i.e. energy of transfer terms, effects associated with the formation of an interface, steric contributions, electrostatic ones, etc.). When interacting polymers are present more terms must be considered [42].

A complete (and realistic) evaluation of the thermodynamic effects responsible for polymer–surfactant interactions is not straightforward; that is why mass-action models are useful. Refined treatments have been presented for this purpose [10–13]. In addition, "small systems thermodynamics" can be used, after rearrangement of the binding equations [14, 15]. This approach may be useful when the number of surfactant molecules interacting with a given polymer binding site is concentration-dependent.

The volumetric findings indicate that the aggregation numbers of PVP-bound micelles are smaller than for free micelles. Accordingly, two equilibria are involved in the system: one related to the binding of aggregates containing <n> units onto a polymer binding site; the second to the formation of micelles containing, on average, <m> surfactant units.

The equations for the surfactant chemical potential at the cac and the cmc*, respectively, are given by

$$\ln(a_{2,1}) - (1/n)\ln(a_{2,n}) = (\mu^0_{2,n} - \mu^0_{2,1})/RT \ , \tag{7}$$

$$(1/n)\ln(a_{2,n}) - (1/m)\ln(a_{2,m}) = (\mu^0_{2,m} - \mu^0_{2,n})/RT \ . \tag{8}$$

Neglecting the activity coefficients, the equilibrium concentration of micellar surfactant, $X_{2,m}$, and of polymer–surfactant complexes, $X_{2,n}$, can be expressed as

$$X_{2,m} = X^m_{2,1}\exp[-m(\Delta\mu^0_{2,m}/KT)] \ , \tag{9}$$

$$X_{2,n} = X^n_{2,1}\exp[-n(\Delta\mu^0_{2,n}/KT)] \ , \tag{10}$$

and can be introduced in the equation for the overall surfactant content, $X_{2,tot}$.

According to Eqs. (7), (8), (9) and (10), the width of the interaction region, keeping the intensive variables fixed, is proportional to the difference between m and n. Such behavior is, indeed, observed in the phase diagrams in Fig. 6.

Fig. 6 Plot of the cac and cmc* lines in pseudobinary diagrams reporting the PVP weight percent as a function of SCAP weight percent at 15 °C (full triangles) and 20 °C. The diagrams for water (dotted line) and for 1 m NaCl at 25 °C are shown in the inset. The partial phase diagram of the water–PVP–TEAPFOSS system at 15 °C (dashed line) and 25 °C, is reported in the triangular diagram

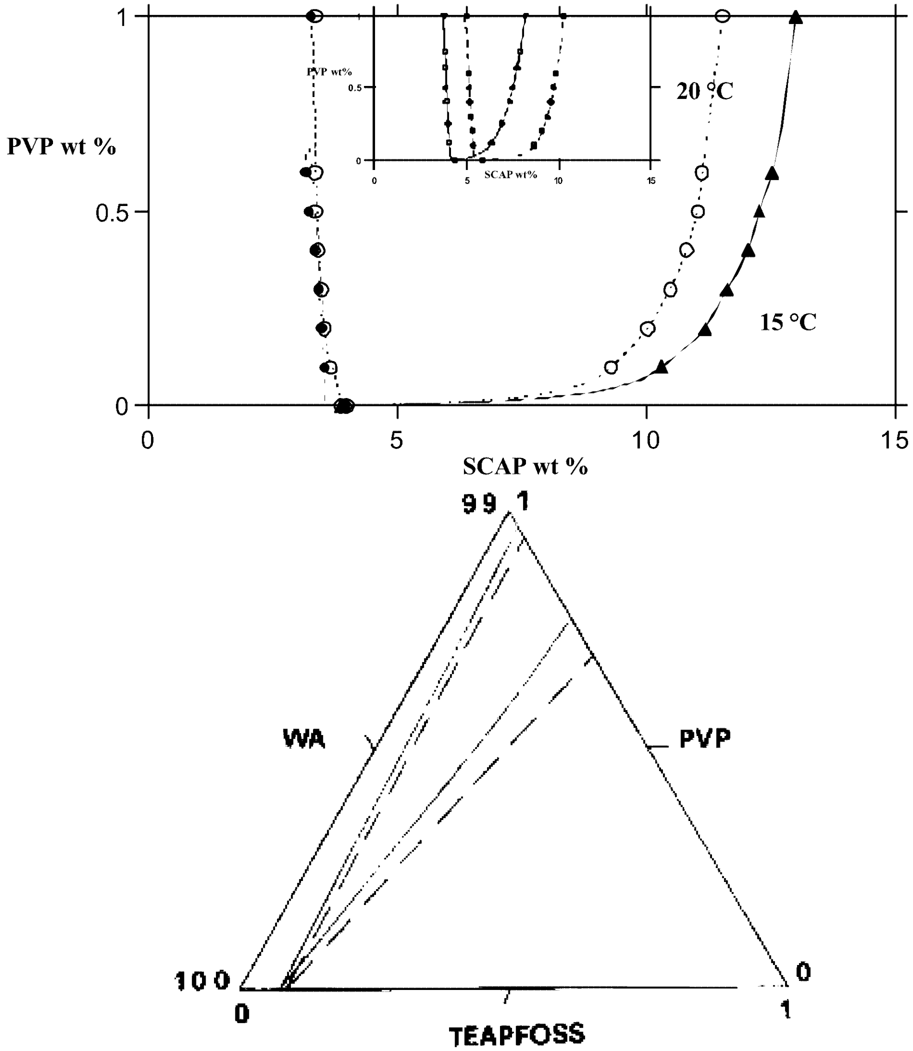

For practical purposes, some data reported there are drawn in pseudobinary plots, others in ternary ones. As can be seen from Fig. 6, the interaction region changes in size and location upon replacement of water with 1 m NaCl. In addition, the width of the aforementioned region decreases on increasing the temperature.

When the overall surfactant concentration, $X_{2,tot}$, is large enough to ensure the occurrence of surfactant monomers, polymer-bound aggregates and free micelles, the following equality holds

$$X_{2,tot} = X_{2,1} + mX_{2,m} + nN_bX_{3,pol}(X_{2,n}/1 + X_{2,n}) \ , \tag{11}$$

where the product $N_bX_{3,Pol}$ is the mole fraction of polymer binding sites in the mixture. (Note, the mass of a binding site is about 2 kDa and N_b is the number of binding sites per polymer molecule.)

If $X_{2,tot}$ is kept fixed, a variation of $X_{3,Pol}$ is concomitant with changes in the distribution of the surfactant in the three different states. In words, $X_{2,1}$, $X_{2,m}$ and $X_{2,n}$ do change. This is reflected in the variation of the cac ($X_{2,1}$) and cmc* ($X_{2,m}$) curves reported in Table 3. The aforementioned $X_{2,1}$ and $X_{2,m}$ curves may be expressed in terms of power-law equations of $X_{3,Pol}$, according to [27, 43]

$$X_{2,m} = X^0_{2,m} + aX_{3,Pol} + bX^2_{3,Pol} + cX^3_{3,Pol} + \dots \ , \tag{12}$$

$$X_{2,1} = X^0_{2,m} + AX_{3,Pol} + BX^2_{3,Pol} + CX^3_{3,Pol} + \dots \ , \tag{13}$$

where a, b, c, ..., and A, B, C, ..., are proper constants. (Note a≠A, b≠B, and so forth.)

When the amount of polymer in the medium, $X_{3,Pol}$, is moderate the equations may be linearized, without loss of generality. In particular, when $X_{2,n}$ is $\ll 1$, Eq. (11) is simplified to

$$X_{2,tot} = X_{2,1} + mX_{2,m} + nN_bX_{3,Pol}X_{2,n} \tag{14}$$

and may be expressed in differential form as

$$(\partial X_{2,\mathrm{tot}}/\partial X_{3,\mathrm{Pol}}) = 0 = (\partial X_{2,1}/\partial X_{3,\mathrm{Pol}}) + \mathrm{m}(\partial X_{2,\mathrm{m}}/\partial X_{3,\mathrm{Pol}}) + \mathrm{nN_b}[\partial(X_{3,\mathrm{Pol}}X_{2,\mathrm{n}})/\partial X_{3,\mathrm{Pol}}] \quad (15)$$

or

$$(\partial X_{2,1}/\partial X_{3,\mathrm{Pol}}) + \mathrm{m}(\partial X_{2,\mathrm{m}}/\partial X_{3,\mathrm{Pol}}) = -\mathrm{nN_b}[X_{3,\mathrm{Pol}}(\partial X_{2,\mathrm{n}}/\partial X_{3,\mathrm{Pol}}) + X_{2,\mathrm{n}}] \ . \quad (16)$$

It must be pointed out that the terms m, n and N_b in Eq. (16) are independent of polymer and surfactant content, because of the constraints dictated by the mass-action law. Equation (16) can be applied to rationalize the phase diagrams reported in Fig. 6. Note that the quantities $(\partial X_{2,1}/\partial X_{3,\mathrm{Pol}})$ and $(\partial X_{2,\mathrm{m}}/\partial X_{3,\mathrm{Pol}})$ are the tangents to the cac and cmc* curves, respectively [44–46]. When the derivatives in Eq. (16) are constant (i.e. when the dependence of $X_{2,\mathrm{m}}$ (and $X_{2,1}$) on the polymer weight percent is nearly linear), an approximate solution can be obtained according to

$$X_{2,\mathrm{n}} = [(\partial X_{2,1}/\partial X_{3,\mathrm{Pol}})^2 + (\partial X_{2,\mathrm{m}}/\partial X_{3,\mathrm{Pol}})^2 - 2X_{3,\mathrm{Pol}}]^{1/2} \approx [\mathrm{a}^2 + \mathrm{A}^2 - 2X^2_{3,\mathrm{Pol}}]^{1/2} \ . \quad (17)$$

Equation (17) can be used in the dilute polymer regime.

The meaning underlying Eq. (17) can be inferred from simple physical considerations. In particular

1. The width of the interaction region at fixed polymer content is controlled by the different affinity of the surfactant for binding compared to the formation of free micelles, i.e. by the Gibbs energy of transfer reported in Fig. 5.
2. The width of the interaction region is related to the difference of average aggregation numbers of free compared to polymer-bound micelles.
3. The temperature and ionic strength modulate the width of the interaction region.

A schematic visualization of the physical meaning of Eq. (17) is sketched in Fig. 7. The scheme shown there can be of use in dilute systems. It must be kept in mind, perhaps, that it gets full thermodynamic meaning when applied to a triangular phase diagram (when the equations for the chemical potential of $X_{1,\mathrm{Wa}}$, $X_{2,\mathrm{tot}}$ and $X_{3,\mathrm{Pol}}$ are considered). Equations (16) and (17) account for some fundamental aspects of polymer–surfactant interactions at low polymer content. For instance, the width of the interaction region is controlled by the polymer affinity with the surfactant.

Equation (17) may explain the differences occurring in the water–PVP–SCAP system compared to the water–PVP–TEAPFOSS one. The shape of the cac and the cmc* curves, in fact, indicates whether ideality conditions are fulfilled. In the low-surfactant-concentration regime the micelles are surely noninteracting and the cmc* curve should be approximately linear. In the water–PVP–TEAPFOSS system, in addition, the unfavorable interactions between fluoromethylene chains and the polymer may imply that polymer-bound micelles do not grow in size. Unfortunately, we do not have direct experimental evidence of such an effect.

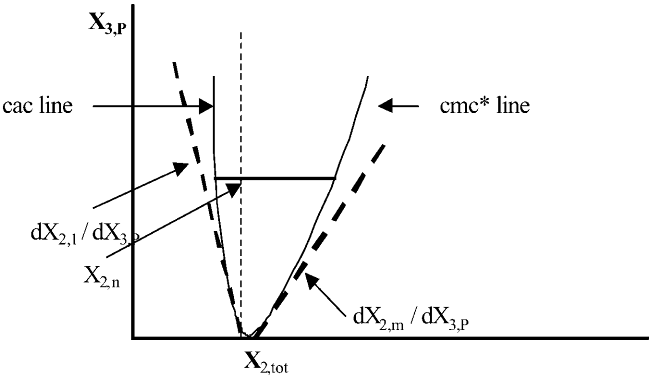

Fig. 7 The links between $X_{2,1}$, $X_{3,\mathrm{Pol}}$, $X_{2,\mathrm{m}}$ and $X_{2,\mathrm{n}}$ in the pseudobinary phase diagrams. The plots are calculated according to Eq. (17)

Modifications in the width of the interaction region owing to the medium ionic strength and/or temperature may be introduced into Eqs. (16) and (17). The effect that temperature exerts on the cac and the cmc* is relatively simple to quantify, for instance.

Polymer–surfactant interactions are not automatically concomitant to micelle formation. Arai et al. [3] and others [47, 48] showed that (at fixed $X_{3,\mathrm{Pol}}$) the cac depends on the surfactant alkyl chain length, C_n, in a similar way as the cmc. Perhaps, the slope of ln(cac) versus C_n may be different from that of the cmc. In some cases, below a critical alkyl chain length, micellization is energetically favored with respect to polymer–surfactant interactions. This is the behavior observed in systems containing PVP and octylsulfate [49]. The physical reasons responsible for the occurrence, or absence, of polymer–surfactant interactions are thus to be ascribed to the overlapping of favorable and unfavorable contributions (electrostatic, solvation, etc.) to the overall stability of polymer-bound aggregates.

Conclusions

The purpose of this contribution was to shed light on the role played by the nature of alkyl chains in polymer–surfactant interactions. Experimental evidence indicates that cac and cmc* values are sensitive to added electrolytes, temperature and polymer content.

Relatively small aggregates (aggregation numbers lower than for free micelles) [6–9] are formed on the polymer binding sites. The determination of aggregation numbers, which had previously been made by different experimental methods [50–53], was estimated by volumetric techniques. In the case of SCAP, the aggregation numbers of polymer-bound aggregates are significantly lower than for free micelles. This is in line with fluorescence decay studies [52].

The application of a mass-action approach to the present systems indicates that the width of the interaction region and the shape of the curves separating the different parts of the phase diagram are controlled by the difference in the number-average aggregation numbers between free and polymer-bound aggregates.

Acknowledgements The Italian Ministry for University, Technical and Scientific Research is acknowledged for financial support, by grant 97 C.F.S.I.B. The authors wish to thank Bianca Sesta, La Sapienza University, for stimulating discussion.

References

1. Jones MN (1967) J Colloid Interface Sci 23:36
2. Jones MN (1968) J Colloid Interface Sci 27:532
3. Arai H, Murata M, Shinoda K (1971) J Colloid Interface Sci 37:223
4. Shirahama K (1974) Colloid Polym Sci 52:978
5. Shirahama K, Ide N (1976) J Colloid Interface Sci 54:450
6. Goddard ED, Ananthapadmanabhan KP (eds) (1992) Interactions of surfactants with polymers and proteins. CRC, Boca Raton
7. Kwak JCT (ed) (1998) Polymer–surfactant systems. Dekker, New York
8. Goddard ED (1986) Colloids Surf 19:255
9. Goddard ED (1986) Colloids Surf 19:301
10. Gilyani G, Wolfram E (1981) Colloids Surf 3:181
11. Nagarajan R (1985) Colloids Surf 13:1
12. Ruckenstein E, Huber G, Hoffmann H (1987) Langmuir 3:382
13. Nikas YJ, Blankschtein D (1994) Langmuir 10:3512
14. Hill TG (1994) Small systems thermodynamics. Dover, Mineola, NY
15. Gilyani G (1999) J Phys Chem B 103:2085
16. Brewer DM, Robb ID (1972) Chem Ind 530
17. La Mesa C, Persi L, D'Aprano A (1998) Ber Bunsen-Ges Phys Chem 102:1459
18. Almgren M, van Stam J, Lindblad C, Li P, Stilbs P, Bahadur P (1991) J Phys Chem 95:5677
19. Thalberg K, Lindman B (1993) Colloids Surf A 76:283
20. Antonietti M, Conrad J (1994) Angew Chem Int Ed Engl 33:1869
21. Moren AK, Khan A (1995) Langmuir 11:3636
22. Moren AK, Khan A (1999) J Colloid Interface Sci 218:397
23. D'Aprano A, La Mesa C, Persi L (1997) Langmuir 13:58
24. Elworthy PH, Mysels KJ (1996) J Colloid Interface Sci 21:331
25. La Mesa C, Ranier GA (1993) Ber Bunsen-Ges Phys Chem 97:620
26. Li Y, Bloor DM, Wyn Jones E (1996) Langmuir 12:4476
27. Desnoyers JE, Perron G (1987) In: Zana R (ed) Surfactant solutions. New methods of investigation. Dekker, New York, p 1
28. Desnojers JE, Caron G, De Lisi R, Roberts D, Roux A, Perron G (1983) J Phys Chem 87:1397
29. La Mesa C, Bonincontro A, Sesta B (1993) Colloid Polym Sci 271:1165
30. Gente G, La Mesa C, Muzzalupo R, Ranieri GA (2000) Langmuir 16:7914
31. Sesta B, D'Aprano A, Segre AL, Proietti N (1997) J Phys Chem B 101:130
32. Persi L, La Mesa C, D'Aprano A (1997) Ber Bunsen-Ges Phys Chem 101:1949
33. Brackman JC, van Os NM, Engberts JBFN (1988) Langmuir 4:1266
34. Brackman JC, Engberts JBFN (1993) Chem Soc Rev 85
35. Singh PP, Anand K, Yanav OP (1990) Indian J Chem Sect A 29:445
36. Ekwall P, Solyom P (1969) Kolloid Z Z Polym 233:945
37. La Mesa C, Sesta B (1987) J Phys Chem 91:1450
38. Campbell AN, Lakshminarayanan GR (1965) Can J Chem 43:1729
39. Herrmann KW (1966) J Colloid Interface Sci 22:352
40. Friman R, Pettersson K, Stenius P (1975) J Colloid Interface Sci 53:90
41. Mukerjee P (1982) J Am Oil Chem Soc 59:573
42. Linse P, Piculell L, Hansson P (1998) In: Kwak JCT (ed) Polymer–surfactant systems. Dekker, New York, p 193
43. Burchfield TE, Woolley EM (1984) J Phys Chem 88:2155
44. Cabane B (1977) J Phys Chem 81:1639
45. Cabane B, Duplessix R (1982) J Phys (Paris) 43:1529
46. Cabane B, Duplessix R (1985) Colloids Surf 13:19
47. Saito S, Taniguchi T, Kitamura K (1971) J Colloid Interface Sci 37:154
48. Saito S, Taniguchi T (1973) J Colloid Interface Sci 44:114
49. Gasbarrone P, La Mesa C (1999) Colloid and Interface Group Italian Chemical Society Meeting, Rome, Italy
50. Lewis KE, Robinson CP (1970) J Colloid Interface Sci 32:539
51. Dong DC, Winnik MA (1982) Photochem Photobiol 35:17
52. Anthony O, Zana R (1996) Langmuir 12:1967
53. La Mesa C (1999) Colloids Surf A 160:37